IVYSPRING INTERNATIONAL PUBLISHER

Theranostics

2017; 7(1): 117-131. doi: 10.7150/thno.17031

Research Paper

# Pre-vascularization Enhances Therapeutic Effects of Human Mesenchymal Stem Cell Sheets in Full Thickness Skin Wound Repair

Lei Chen[1,#], Qi Xing[3,#], Qiyi Zhai[1], Mitchell Tahtinen[3], Fei Zhou[1], Lili Chen[2], Yingbin Xu[1], Shaohai Qi[1,✉], Feng Zhao[3,✉]

1. Department of Burns, First Affiliated Hospital of Sun Yat-sen University, Guangzhou, China
2. Department of Pathology, First Affiliated Hospital of Sun Yat-sen University, Guangzhou, China
3. Department of Biomedical Engineering, Michigan Technological University, Houghton, Michigan, USA.

[#] Equal contribution

✉ Corresponding author: Feng Zhao, Department of Biomedical Engineering, Michigan Technological University, 1400 Townsend Drive, Houghton, MI 49931, U.S. Tel: 906-487-2852; Fax: 906-487-1717; Email: fengzhao@mtu.edu. Shaohai Qi, Department of Burns, The First Affiliated Hospital of Sun Yat-sen University, Guangzhou, 510080, China. Email: qishaohaigzburns@163.com.



Received: 2016.07.29; Accepted: 2016.09.29; Published: 2017.01.01

## Abstract

Split thickness skin graft (STSG) implantation is one of the standard therapies for full thickness wound repair when full thickness autologous skin grafts (FTG) or skin flap transplants are inapplicable. Combined transplantation of STSG with dermal substitute could enhance its therapeutic effects but the results remain unsatisfactory due to insufficient blood supply at early stages, which causes graft necrosis and fibrosis. Human mesenchymal stem cell (hMSC) sheets are capable of accelerating the wound healing process. We hypothesized that pre-vascularized hMSC sheets would further improve regeneration by providing more versatile angiogenic factors and pre-formed microvessels. In this work, *in vitro* cultured hMSC cell sheets (HCS) and pre-vascularized hMSC cell sheets (PHCS) were implanted in a rat full thickness skin wound model covered with an autologous STSG. Results demonstrated that the HCS and the PHCS implantations significantly reduced skin contraction and improved cosmetic appearance relative to the STSG control group. The PHCS group experienced the least hemorrhage and necrosis, and lowest inflammatory cell infiltration. It also induced the highest neovascularization in early stages, which established a robust blood micro-circulation to support grafts survival and tissue regeneration. Moreover, the PHCS grafts preserved the largest amount of skin appendages, including hair follicles and sebaceous glands, and developed the smallest epidermal thickness. The superior therapeutic effects seen in PHCS groups were attributed to the elevated presence of growth factors and cytokines in the pre-vascularized cell sheet, which exerted a beneficial paracrine signaling during wound repair. Hence, the strategy of combining STSG with PHCS implantation appears to be a promising approach in regenerative treatment of full thickness skin wounds.

Key words: skin graft, human mesenchymal stem cell, prevascularized cell sheet, angiogenic growth factors

## Introduction

Burns are one of the major causes of full thickness skin wounds. There are approximately 15,000–20,000 hospitalizations per year for acute burn injuries in the U.S., as recorded by the American Burn Association [1]. Despite the fact that numerous approaches and skin substitutes have been developed for burn treatment, the current golden standard consisting of autologous skin full thickness grafts

(FTG) or skin flap transplantation is still considered a safe, effective, and economically viable method for restoring permanent coverage [2]. FTG and skin flaps have numerous advantages over engineered materials, including immunological acceptance as well as color and texture match. However, an inadequate supply of donor skin and the unavoidable donor site injury seriously limit their potential to treat extensive and severe wounds.

One promising solution is the application of an autologous split thickness skin graft (STSG). Although donor sites need re-epithelialization and have an ongoing wound therapy requirement until repaired, these sites may be harvested repeatedly to resurface large wounds. STSG can be used under unfavorable conditions, such as a recipient's wound having moderate infection or less vasculature, where FTG would fail [3]. However, STSG are more fragile than FTG and can contract significantly during the healing process. Combined transplantation of STSG with engineered dermal substitutes could overcome the disadvantages of STSG transplantation, such as contracture, poor cosmetic outcome, physical disability, and reduced pliability [4]. Nevertheless, due to an insufficient blood supply at early stages of the transplantation, these skin grafts suffer a relatively long hypoxic and ischemic period after surgery and suffer from degeneration and necrosis [5]. While bio-engineered products such as natural substitutes - human allograft, Oasis wound matrix®; synthetic substitutes - Biobrane™; permanent skin substitutes - Epicel®, and Integra® have been commercially available for years, major problems still exist with material sources, manufacturing techniques, material compatibility, and therapeutic effects [6]. Hence, a new strategy with better therapeutic effects is still critically needed.

Cell-based therapies, especially those using stem cells, for improving survival and the therapeutic effect of skin grafts, have emerged as a new approach in recent years [7]. Mesenchymal stem cells (MSCs) exhibit excellent potential for accelerating wound healing due to their self-renewal ability, secretion of paracrine factors, and ability to differentiate into different cell lineages [8]. Numerous studies reported positive results when utilizing MSCs for various wound regeneration applications [9-12]. Local delivery of rat adipose-derived MSCs to an excisional wound healing model showed enhanced epithelialization and granulation tissue deposition [13]. Human MSCs (hMSCs) grafted in impaired healing diabetic mice significantly improved healing by recruiting large amounts of host mouse MSCs to the wound bed, producing signals such as vascular endothelial growth factor (VEGF) and platelet-derived growth factor receptor-α (PDGFR-α) [14]. Compared to traditional cell delivery strategies, such as cell injection or spraying, cell sheet engineering techniques enhance the cell delivery efficacy to injured tissue [15]. The cell sheet preserves cell-cell junctions, extracellular matrix (ECM), and cell-matrix connections thus restricting the cells to the wound bed [16]. The rat adipose-derived MSC sheet demonstrated beneficial effects in diabetic wound healing when combined with artificial skin, where the cells accelerated wound healing directly by functioning as pericytes and indirectly through the secretion of paracrine signaling factors [17].

Whether or not the skin graft has a sufficient blood supply is the primary factor that influences the quality of transplanted STSGs [18]. During the first 48 hours of transplantation, the graft is engorged by plasmatic fluid and a poorly vascularized bed hinders plasmatic diffusion [18]. In addition, newly formed blood vessels in the wound bed can deliver oxygen, nutrients, and essential growth factors to hypoxic and ischemic STSGs at early stages after placement [19]. Pre-formation of microvessels on cell sheets may enhance angiogenesis as well as further improve tissue function by supporting cell survival and accelerating its integration with host tissues. For example, a pre-vascularized bone graft implanted subcutaneously in nude mice demonstrated a much higher density of microvessels *in vivo* than a non-vascularized bone graft. In addition, more bone matrix was found in the pre-vascularized samples [20]. A pre-vascularized cardiac patch grafted to a rat heart showed an increased number of new patent blood vessels than its avascular counterpart. These new microvessels consisted of both donor and host-derived vasculatures [21]. Among all cell types used for angiogenesis and neovascularization, the role of endothelial cells (ECs) has been studied extensively. They are able to initiate postnatal neovascularization and express a series of growth factors and cytokines including platelet derived growth factor (PDGF), transforming growth factor (TGF)-$\beta$, granulocyte-macrophage colony-stimulating factor (GM-CSF), interleukin-1 (IL-1), IL-5 and IL-6, which are beneficial for wound repair [22]. When co-cultured with hMSCs, the formation of a microvessel network is promoted due to the supporting and stabilizing functions of hMSCs [23]. Cross-talk between ECs and hMSCs up-regulates the expression of genes such as von Willebrand factor (vWf), platelet/endothelial cell adhesion molecule-1 (PECAM-1), and cadherin 5 [24]. Furthermore, EC/hMSC cross-talk has been shown to improve angiogenesis via synergistic effects [25]. Therefore, an hMSC cell sheet (HCS) co-cultured with ECs may

facilitate neovasculature formation and improve skin graft survival.

The purpose of this work was to evaluate the efficacy of a novel engineered pre-vascularized hMSC cell sheet (PHCS) transplanted in combination with an autologous STSG to promote vascularization and healing in a rat full thickness wound model. The hMSC sheets were first cultured under hypoxic conditions (2% $O_2$) and then co-cultured with ECs under normoxic conditions (20% $O_2$) in order to improve the uniformity of cell sheet and microvessel network formation [26]. Human umbilical vein endothelial cells (HUVECs), typical ECs that are normally used as model cells in studies of microvessel assembly *in vitro*, were selected to examine the effect of the PHCS on skin wound healing. The amount of various growth factors in both HCS and PHCS were quantified. The function and multi-potency of hMSCs in the cell sheets were analyzed. The wound healing effects of cell sheets/STSG grafts were evaluated at different time points up to 28 days by characterizing wound contraction, epidermis thickness, collagen deposition, neovasculature density, and skin appendage recovery. We aimed to establish a new cell-assisted and pre-vascularized method to improve the STSG repairing effects.

## Materials and Methods

### Preparation of hMSC cell sheet (HCS) and pre-vascularized hMSC cell sheet (PHCS)

Cell sheet culture followed the method in our previous publication [26]. The culture conditions of hMSC sheet and pre-vascularized hMSC sheet were optimized in order to enhance the cell sheet strength and microvessel length and branch. Briefly, passage 3 to 5 hMSCs (Texas A&M University Health Sciences Center) were seeded on cover glasses coated with 20 μg/mL collagen I (BD Biosciences, San Jose, CA) at a density of 10,000 cells/cm$^2$. The hMSCs were cultured under a hypoxic condition (2% $O_2$) for 4 weeks to obtain HCS in *a*-minimum essential medium with 20% fetal bovine serum, 1% L-glutamine and 1% penicillin/streptomycin (Life Technologies, Rockville, MD). The hMSC sheets with a diameter of 2 cm were harvested by gently peeling the cell layers off the cover glass [26]. The thickness of detached hMSC sheets and ECM scaffolds (fixed using 4% paraformaldehyde (PFA)) was measured using an Olympus FV1000 confocal microscope. Six samples were used for the measurement. To prepare the pre-vascularized hMSC sheet, HUVECs (Lonza, Walkersville, MD) were seeded on top of hMSC sheets at a density of 20,000 cells/cm$^2$ and cultured under a normoxic condition (20% $O_2$) for 1 week to obtain PHCS in endothelial cell growth medium (EGM-2, BulletKit, Lonza). The medium was changed every other day.

### Immunofluorescence staining and microvessel quantification

The microvessel formation on hMSC sheets was examined by immunofluorescence staining. The cell sheets were washed with phosphate-buffered saline (PBS), fixed with 4% PFA, permeabilized with 0.2% Triton X-100 in PBS, blocked with 1.0% bovine serum albumin (Thermo Fisher Scientific, MA) in 0.2% Triton X-100, and incubated with the primary CD 31 antibody (Abcam, Cambridge, MA). Then the samples were incubated with DyLight 488 secondary antibody (VECTOR Laboratories, CA). The 4′, 6-diamidino-2-phenylindole (DAPI, Sigma, St. Louis, MO) solution was used to stain the cell nuclei. Images were visualized under an Olympus BX-51 fluorescence microscope. The microvessels were quantified following the method in our previous publication [26]. The average diameter of microvessels and the length of microvessels per unit area were calculated using ImageJ. Six low-magnification (20X) images of microvessel networks on three individual samples in each group were used for calculation.

### Growth factor assay

The angiogenic growth factor amount present in the cell sheets was analyzed using an enzyme-linked immunosorbent assay (ELISA). Growth factors embedded in the HCS were extracted as previously described [27]. Briefly, each cell sheet was soaked in 1 mL urea-heparin extraction buffer consisting of 2 M urea and 5 mg/mL heparin in 50 mM Tris with protease inhibitors [1 mM Phenylmethylsulfonyl Fluoride (PMSF), 5 mM Benzamidine, and 10 mM N-Ethylmaleimide (NEM)] at pH 7.4. The extraction mixture was rocked at 4 °C for 24 h and then centrifuged at 12,000 g for 30 min at 4 °C and the supernatants were collected. Microvessel formation related growth factors TGF-β1, VEGF, Angiopoietin 1 (ANG1), Angiopoietin 2 (ANG2), and basic fibroblast growth factor (bFGF) were determined using ELISA kits (R&D Systems, Minneapolis) according to the manufacture's instruction. In each experiment, three identical samples of each condition were examined and all samples and standards were measured in duplicate.

### Colony-forming unit-fibroblast (CFU-F) assay

To determine CFU-F numbers, hMSCs were harvested aseptically from 4-week HCS using a solution containing 0.5% trypsin - 0.25% collagenase-1 mmol/L EDTA in PBS. Cells were filtered using a cell

strainer to ensure cell separation, and 800 cells were plated into a 10 cm petri dish (14 cells/cm$^2$). The cells were grown for 12–14 days at 37 °C and 5% $CO_2$ in a humidified incubator. Cells were washed with PBS and stained with a 0.5% crystal violet solution for 10 minutes at room temperature. Cells were washed twice with PBS and imaged with a digital camera. The visible, intensely stained colonies with more than 40 cells were counted. hMSCs before seeding were employed as control. Six identical petri dishes were employed for calculation in each condition.

### Multi-lineage differentiation assays

To examine the multi-differentiation ability of hMSCs inside the cell sheet after long-term co-culture with ECs, differentiation was performed on the HCS and PHCS. The cell sheets were cultured in osteogenic-inducing medium or adipogenic-inducing medium for 14 days following a method reported previously [28]. The osteogenic-inducing medium is composed of hMSC culture medium supplemented with 10 nM dexamethasone, 20 mM β-glycerolphosphate, and 50 μM L-ascorbic acid 2-phosphate. The adipogenic-inducing medium is composed of hMSC culture medium supplemented with 0.5 μM dexamethasone, 0.5 μM isobutylmethylxanthine, and 50 μM indomethacin. Von Kossa staining and calcium deposition were performed to characterize the mineralization of ECM in osteogenic-induction culture according to previously published methods [29]. At the same time points, the lipid vacuoles in adipogenic-induction culture were stained by Nile red and quantified by oil red o assay as described previously [30]. The quantitative results were obtained by analyzing three identical samples in each condition.

### Animals

All experimental procedures were approved by the First Affiliated Hospital of Sun Yat-sen University Institutional Animal Care and Use Committee. The Sprague Dawley (SD) rats (weighing 180-200g) were obtained from the Experimental Animal Center of Sun Yat-sen University. All efforts were made to minimize animal suffering and the number of rodents utilized in this study. The animals were divided into three groups according to the different grafts applied to the wound bed: STSG, STSG with HCS, and STSG with PHCS. SD rats were randomly assigned to one of the three groups, with 30 rats in each group.

### Full thickness excision wound creation and graft transplantation

All rats were anesthetized with inhaled gas anesthesia ($O_2$, 2 L/min; isoflurane, 2%) prior to surgery. The dorsal skin of the rat was scrubbed with Betadine Veterinary Surgical Scrub and 70% alcohol, and a round full-thickness excisional wound with a diameter of 20 mm was created on the rat dorsum by using iris scissors under sterile surgical conditions. The STSG graft was obtained by removing the deep partial dermis as well as panniculus carnosus away from the excised skin [31, 32]. Evenly spaced fenestrations were made on the grafts by use of a sharp tipped scalpel for secretion drainage. After transplanting three cell sheets on each wound, the autologous STSG was laid on top of the cell sheet. The STSG transplantation without a cell sheet was used as control. The grafts and adjacent wound margin were approximated and sutured with interrupted stitches. A padded bolster was then applied on top of the skin grafts to provide appropriate pressure and prevent scratching. All animals were housed in individual cages after surgery. Dressings were changed on postoperative day 3 and removed on day 7. The wounds were observed at days 0, 3, 7, 14, 21, and 28 post-surgery. The skin grafts contraction were measured by gravitational planimetry and expressed as a percentage of the remaining skin graft size to its original wound size by using the following formula:

$$Relative\ skin\ graft\ size\ \% = \frac{Remaining\ skin\ graft\ size}{Original\ skin\ graft\ size} \times 100\%$$

### Tissue collection

Rats were sacrificed at predetermined time points (six rats in each group for each time point). The grafts and surrounding tissues were harvested and divided into two parts along the centerline. All samples were fixed in 10% formalin at room temperature, followed by dehydration through a graded series of ethanol wash, and then embedded in paraffin.

### Pathology analysis: staining, imaging, and analysis

After dewaxation and rehydration, tissue sections with 5 $\mu$m thickness were used for staining. Hematoxylin and eosin (HE) staining, Masson's Trichrome staining, and Toluidine blue staining were performed following the manufacturer's (Sigma) standardized protocols. Immunohistochemistry (IHC) Ki67 and NM95 staining was proceeded using established methods [33]. Measurements of epidermal thickness [34], collagen index [35], and microvessels, hair follicles and cell counting [36-38] in high-power field (HPF) were performed with ImageJ software. The vessel area, which is defined as the sum of all vessel segments/HPF, was quantified by ImageJ using the technique described previously [39]. Five

stained sections in each group for each time point were visualized using an Olympus IX71 microscopy, and three random views in each section were selected for quantitative assay.

### Statistics/data analysis

The results were reported as mean ± standard deviation. Statistical comparisons between conditions were performed using either one-way ANOVA or Student's t-test when appropriate. Results were considered statistically significant for $p < 0.05$.

## Results

### Characterization of hMSC cell sheets (HCS) and pre-vascularized hMSC cell sheets (PHCS)

After 4-weeks of culture under hypoxic conditions (2% $O_2$), a HCS with a thickness of 10.71 ± 0.16 μm was formed. ECs were then seeded on top of the HSC and co-cultured at 20% $O_2$ for 1 week to form the PHCS. Branched microvessels on the cell sheets are shown in Figure 1A. The average diameter of the microvessels was 11.9 ± 0.89 μm. The average length of the microvessels was 12.5 ± 0.88 mm per $cm^2$. Both HCS and PHCS contained various growth factors. Regarding our research objective, the total levels of cytokines in the cell sheet were characterized since the entire cell sheet was implanted. As shown in Figure 1B, different angiogenic growth factors were assayed including VEGF, bFGF, TGF-β1, ANG1, and ANG2. Both VEGF and bFGF are capable of stimulating new blood vessel formation [40]. TGF-β1 is reported as a pro-angiogenic factor that improves EC migration and proliferation or vessel maturation [41]. ANG1 is recognized in promoting vessel stabilization and tightness through stimulating mural coverage and basement membrane deposition [42]. ANG2 is mainly secreted by ECs at sites of active vascular remodeling [43]. The VEGF amount in HCS was around 4.4 times higher than that in PHCS ($p < 0.05$). The bFGF amount in both cultures was comparable ($p > 0.05$). The TGF-β1 amount in PHCS was slightly higher than HCS, but there was no significant difference ($p > 0.05$). The ANG1 amount in PHCS was around 2.6 times higher than in HCS ($p < 0.05$). The ANG2 amount in PHCS was also high, but there was no detectable level of ANG2 in HCS.

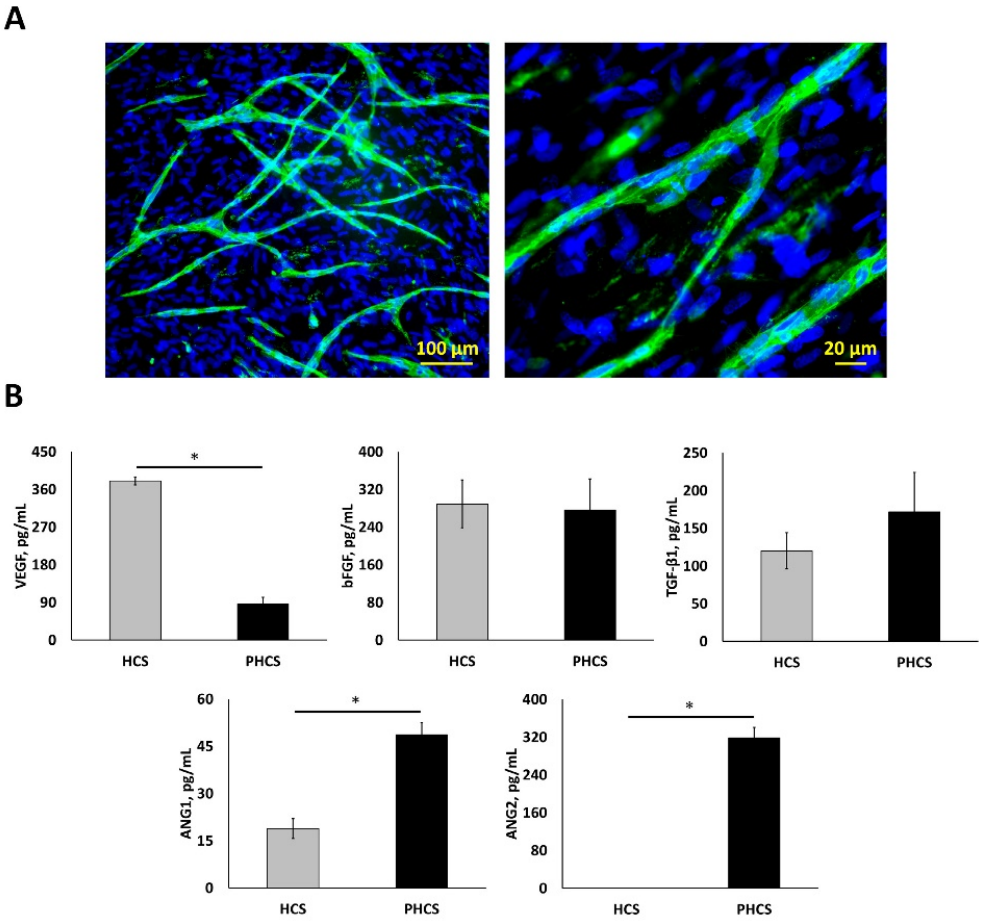


**Figure 1.** Characterization of hypoxic HCS and PHCS. (A) Morphology of microvessels on PHCS at different magnification. Blue: nucleus stained by DAPI; green: microvessels stained by CD31. (B) Growth factor expression in HCS and PHCS. *$p < 0.05$. PHCS group had more growth factors than HCS.

### Progenitor population and multi-lineage differentiation ability of hMSCs

By measuring the colony-forming ability of the cells, we were able to determine the proportion of primitive cells in the cell sheet. As indicated by Figure 2A, the hMSCs before seeding were able to form much more colonies (98 ± 6 colonies) than the hMSCs extracted from HCS (46 ± 2 colonies). Although the progenitor population significantly decreased ($p < 0.01$), around half of the hMSCs maintained self-renewal capacity after extended periods of culture. Osteogenic and adipogenic differentiation assays were performed to determine whether the cells in HCS or PHCS maintained multi-lineage differentiation capabilities. In osteogenic differentiation medium, both cell cultures produced mineralized ECM stained positively by von Kossa (Figure 2B), and quantitative calcium deposition assay showed that PHCS contained much higher calcium than HCS ($p < 0.05$). In adipogenic differentiation medium, both cell cultures contained lipid droplets, stained green by Nile red (Figure 2C), and quantitative oil red o assay showed that HCS and PHCS had comparable adipogenic differentiation capacity ($p > 0.05$).

### Skin grafts contraction

Skin graft contraction in rats treated with STSG, HCS, or PHCS was studied over 28 days. The representative images of skin grafts at different time points are shown in Figure 3A. While PHCS skin grafts became flat, furry, and colored, grafts in the STSG and HCS groups were still reddish, exhibiting un-desquamated crusts, a sign of local ulceration and unstable, immature graft take. The relative skin graft size was expressed as the percentages of remaining skin graft size to its original size. Small remaining skin graft size indicated severe graft contraction causing skin constriction and abnormal morphology which

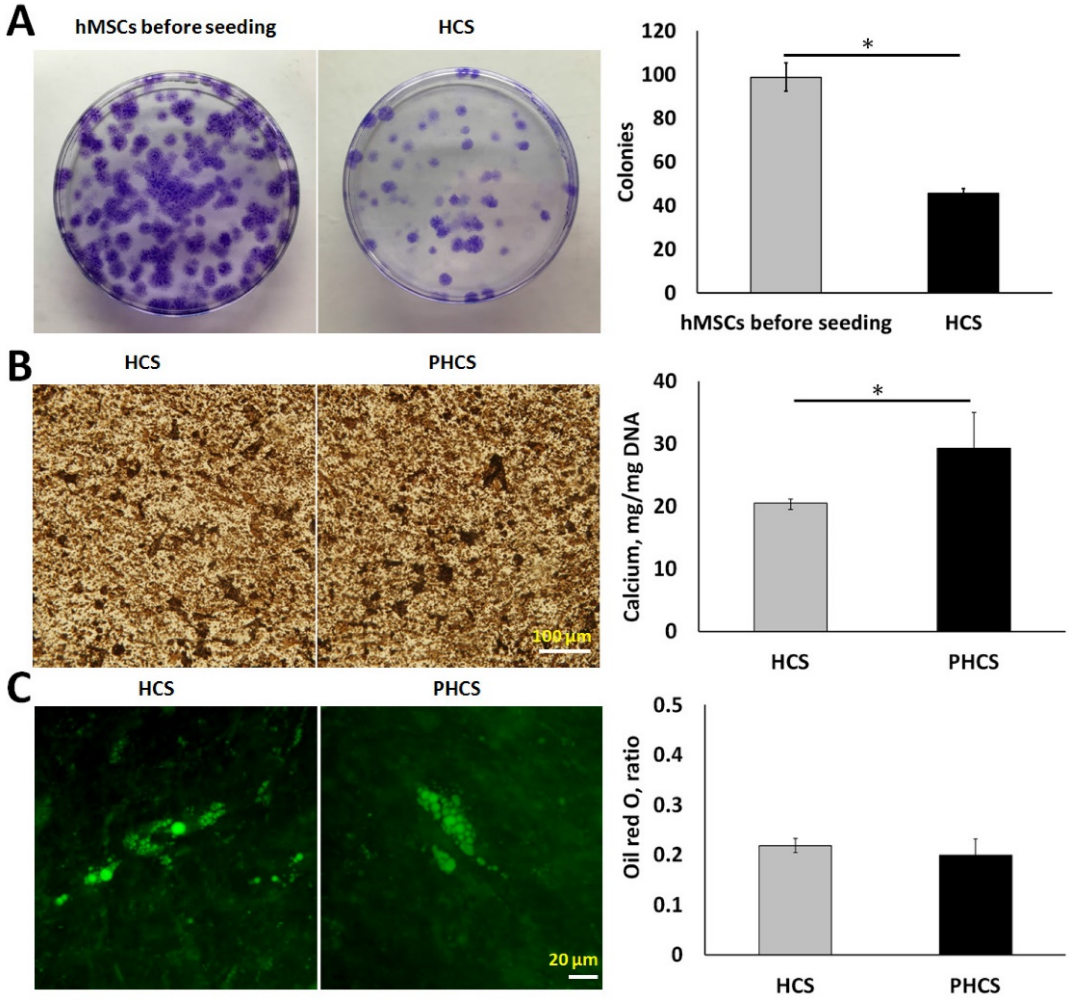


**Figure 2.** Progenicity and multi-lineage differentiation ability of hMSCs in HCS and PHCS. (A) Morphology and quantification of colonies formed by hMSCs before seeding and cells extracted from HCS. *$p < 0.05$. (B) Von Kossa staining of mineralized ECM and calcium deposition in osteogenic-differentiated HCS and PHCS. (C) Nile red staining of lipid vacuoles and oil red o quantification in adipogenic-differentiated HCS and PHCS. The cells in HCS and PHCS maintained a certain degree of progenicity and multi-lineage differentiation ability.

may affect normal skin function. Although partial skin grafts necrosis or ulcers were noticed in some of the STSG or HCS rats, there were no significant differences among the groups at day 3 and day 7 after surgery ($p > 0.05$). The PHCS significantly inhibited the contraction of grafts relative to the control or the HCS ($p < 0.05$, Figure 3B), as proved by a much larger skin graft in PHCS treated rats compared with the control and HCS groups on day 14 (80.14 ± 2.56% vs. 63.72 ± 3.79% and 72.72 ± 0.60%, respectively, $p < 0.05$). The greatest difference in the relative graft size was observed at day 28 and the relative graft size of the PHCS group (67.64 ± 3.69%) was 2.55-fold larger than that of the STSG group (26.58 ± 1.98%, $p < 0.05$) and 1.44-fold larger than that of the HCS group (47.11 ± 2.62%, $p < 0.05$).

## Skin graft survival and alterations of skin appendages

HE analysis was performed to evaluate microstructural and cellular changes within the grafts. As shown in Figure 4A, at day 3, the grafts from STSG and HCS groups were thin with many necrotic foci, and sebaceous glands were missing. The grafts from PHCS groups preserved most skin appendages and supporting loose connective tissues. In addition, large areas of hemorrhage were observed in the STSG group. The HCS group showed moderate hemorrhage. No obvious hemorrhage was observed in the PHCS group (Figure S1). Besides hemorrhage, inflammatory cells were observed to have infiltrated into the grafts of the STSG group and surrounding degenerate or coagulation necrosis hair follicles, forming a ribbon-shaped structure in the dermis of the grafts. Whereas the HCS and PHCS groups showed fewer inflammatory cells (Figure S1). The inflammatory response in STSG grafts was decreased at day 14 and a large number of fibroblasts and conglomerate scar tissue were found in the dermal layer. By day 14, the inflammatory response in HCS

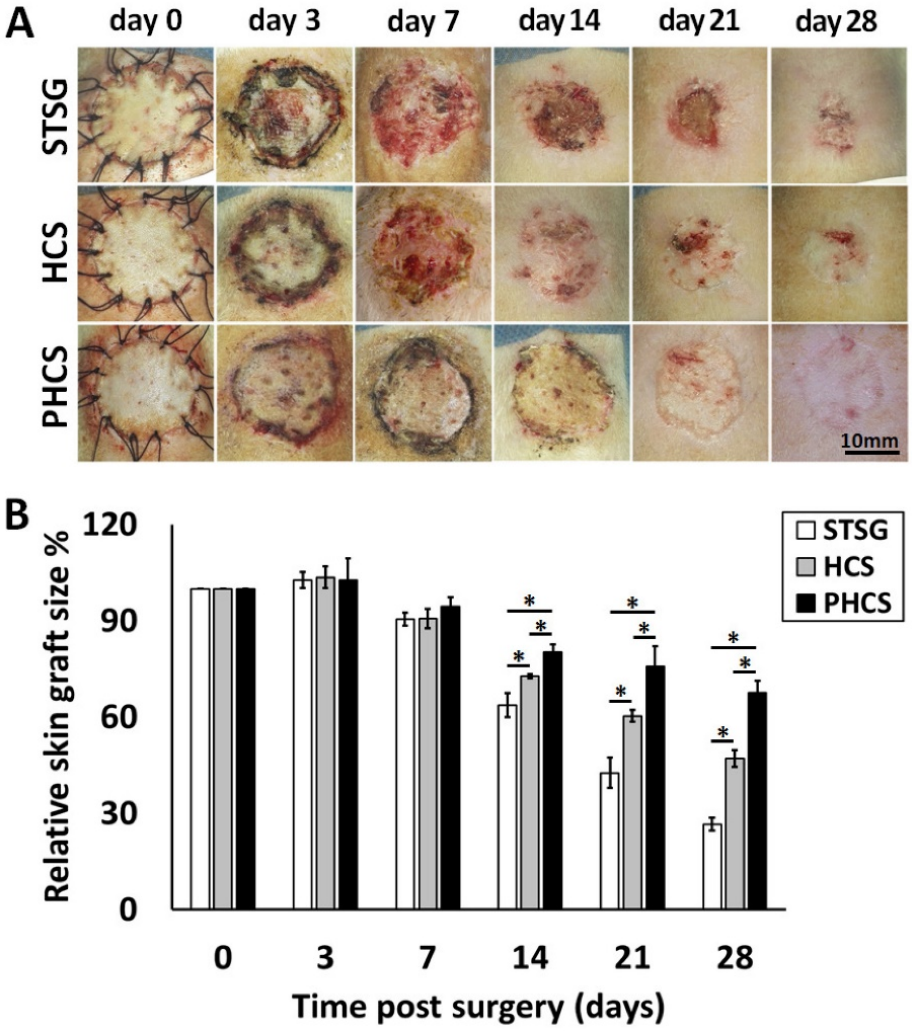


**Figure 3.** Contraction of different skin grafts: STSG, HCS, and PHCS. (A) Morphology of skin grafts over 28 days post surgery. (B) Quantification of relative skin graft size. *$p < 0.05$. Grafts of STSG groups had contracted to 27% of their original size by day 28, whereas PHCS group remained 68% of the initial graft size.

and PHCS grafts was reduced significantly. The prolonged recruitment and presence of mast cells and macrophages at the site of tissue repair could result in fibrosis [44]. Toluidine blue staining was used for detection of mast cells (Figure S2). At day 3, the number of mast cell in HCS (10.40 ± 0.51/HPF) and PHCS (7.00 ± 0.71/HPF) groups was much higher than that of STSG (3.60 ± 0.51/HPF, $p < 0.05$). While at later stages the mast cell number dramatically increased in the STSG (day 14: 15.20 ± 0.66/HPF; day 28: 10.40 ± 1.33/HPF), which was significantly higher than the other two groups ($p < 0.05$). The mast cell number in HSC and PHCS groups gradually decreased from day 3 to day 28, with the PHCS group having the lowest mast cell number.

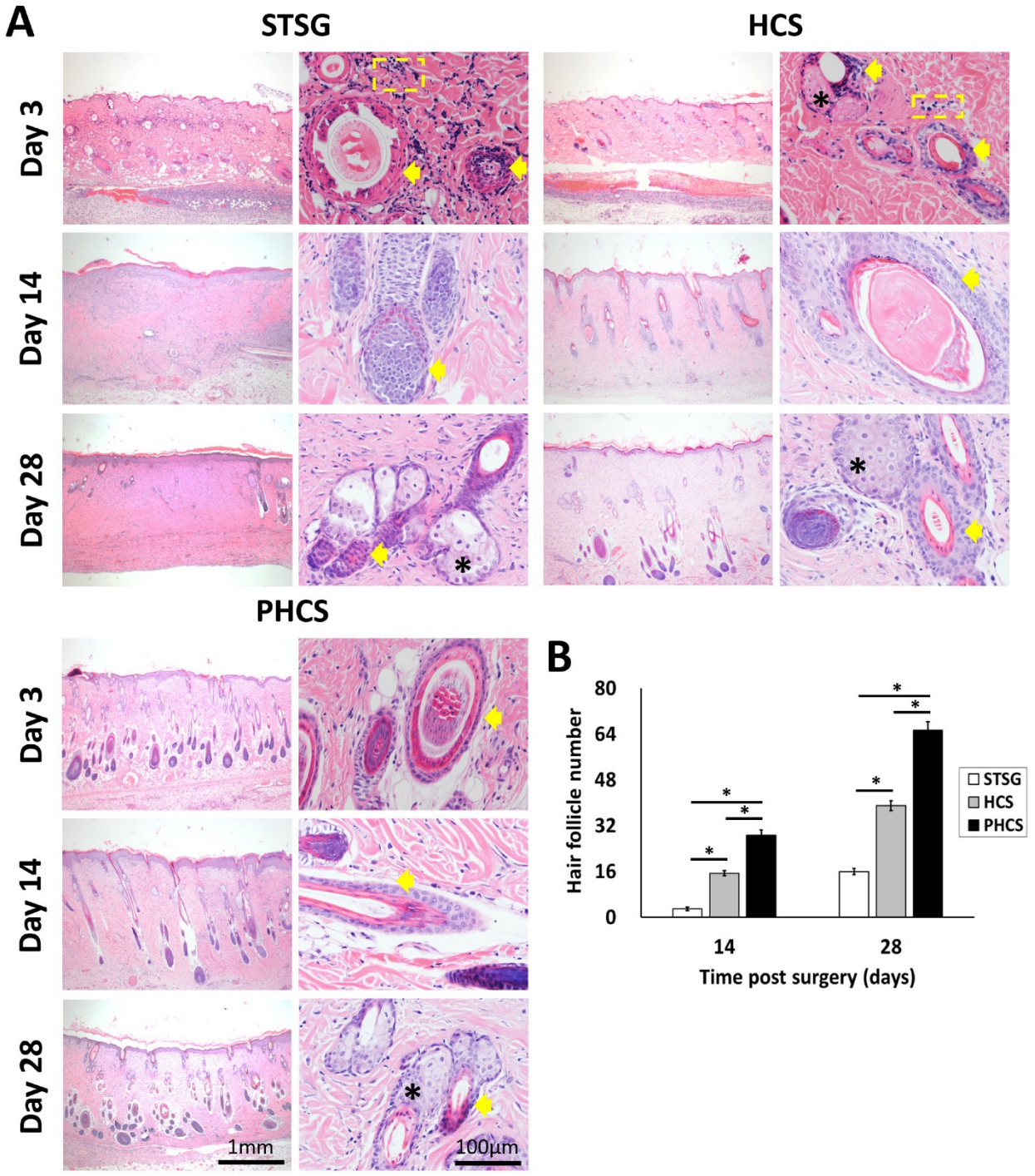


**Figure 4.** The alteration of skin appendages in different grafts. (A) HE staining of epidermis section showing hair follicles (indicated by yellow arrows), sebaceous glands (black stars), and neutrophils (yellow dashed rectangles). (B) Quantification of hair follicles. *$p < 0.05$. The PHCS group better preserved and recovered skin appendages.

The hair follicles in the dermal layer were counted as shown in Figure 4B. Only a few hair follicles (3.00 ± 0.58) were seen in the STSG group at day 14. On the contrary, the distribution of hair follicles in the PHCS group was more even than in the HCS grafts. The number of hair follicles/HPF was also significantly higher than that of HCS grafts ($p < 0.05$). While sebaceous glands and hair follicles were still rare in STSG at day 28, HSC and PHCS grafts preserved significantly higher amounts of skin appendages. The number of hair follicles/HPF in PHCS grafts (65.33 ± 2.96) was significantly higher than that in the STSG (16.00 ± 1.15) and HCS grafts (39.00 ± 1.73) ($p < 0.05$).

## Epidermis morphological changes in skin grafts

The morphology and thickness of the epidermis were characterized in Figure 5. At day 3, the epidermis of the STSG group was atrophic and thin. While HCS and PHCS groups had a thicker epidermis layer with more epithelial cells. At day 14, the epidermal wound repair was completed in all experimental groups. A noticeable increase was found in the epidermal thickness of all grafts (STSG: 114.39 ± 6.33 μm, HCS: 74.20 ± 3.29 μm, PHCS: 61.16 ± 2.84 μm). From day 14 to day 28 the epidermis thickness did not change significantly, with that of the PHCS grafts (55.24 ± 0.79 μm) being closest to the normal skin (37.34 ± 1.68 μm). The epidermis thickness of STSG group is much higher than all the other groups at both day 14 and day 28.

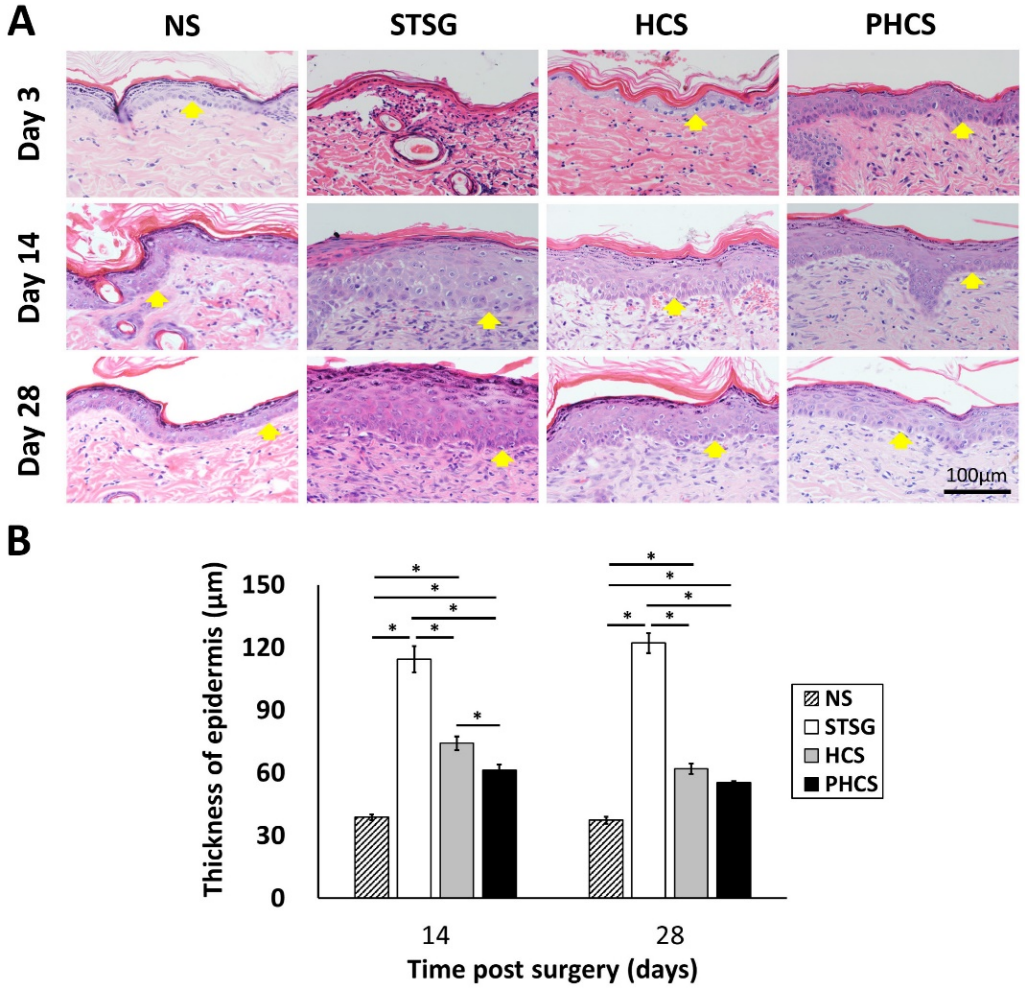


**Figure 5.** Characterization of epidermis in different grafting groups and normal skin (NS). (A) HE staining of epidermis. Yellow arrows show the position of epidermis. (B) Thickness of epidermis on day 14 and 28. *$p < 0.05$. The PHCS group had the least amount of skin fibrosis and the epidermis thickness was close to that of normal skin.

### Cellularity and vascularization of skin grafts

NM95 staining was applied to determine whether implanted human cells (hMSCs and ECs) actually participated in the process of skin wound healing after grafting. NM95-postive cells were only found at day 3 in the HCS group (Figure S3). A small percentage of NM95 positive cells were found incorporated into the epidermis, hair follicles, and microvessel like structures. Therefore, most of the cells present in the wound area were originated from rats. The cell proliferation in the granulation tissue was accessed by staining Ki67, a nuclear antigen expressed in proliferating cells, shown as a brown color in Figure 6 A and B. During the three stages of wound healing - inflammation, proliferation, and maturation, different types of cells are involved and proliferating at different stages, including inflammatory cells, fibroblasts, endothelial cells, and keratinocytes [45]. Composed largely of inflammatory cells and fibroblasts, STSG grafts showed a much higher number of proliferating cells at day 3 compared to HCS and PHCS grafts (STSG: 128.80 ± 2.96/HPF, HCS: 92.40 ± 2.87/HPF, PHCS: 74.20 ± 3.65/HPF). A significant drop in cell proliferation was seen at day 14 (STSG: 73.20 ± 2.33/HPF, HCS: 39.20 ± 2.06/HPF, PHCS: 25.40 ± 3.44/HPF) ($p < 0.05$), with the lowest number of proliferating cells being found in the PHCS group.

The HE staining of the granulation tissue showed the microvessel morphology, numbers, and area (Figure 6 C, D and E). The microvessels were clearly seen in all grafts with the presence of blood cells inside the lumen. At day 3, the microvessel number in the STSG group (6.80 ± 0.97/HPF) was much lower than HCS (16.00 ± 0.71/HPF) and PHCS groups (22.00 ± 1.30/HPF) ($p < 0.05$). While the vessel number significantly increased in the STSG group up to day 14 (30.20 ± 1.59/HPF) and day 28 (32.00 ± 1.58/HPF) ($p < 0.05$), the number of vessels in HSC and PHCS grafts increased slightly at day 14 (23.00 ± 1.41/HPF vs. 24.20±1.32/HPF) but decreased at day 28 (20.60 ± 0.75/HPF vs. 11.40 ± 1.03/HPF). The decreasing trend was more evident in the PHCS grafts. By day 28, the vessel numbers in HCS and PHCS groups were significantly lower than the STSG group ($p < 0.05$). The microvessel area quantification also showed the degree of graft vascularization from

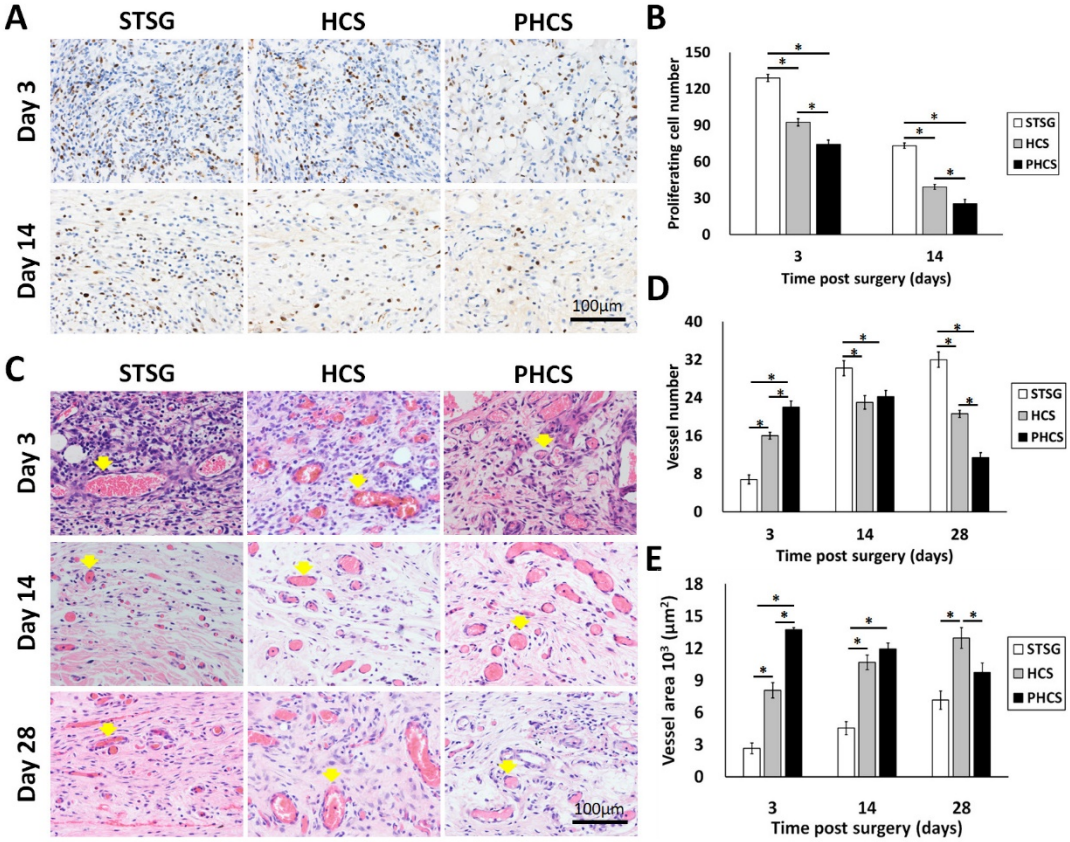


**Figure 6.** Characterization of granulation tissue underneath the skin graft. (A) Ki 67 staining of proliferating cells. Blue: cell nucleus; brown: Ki67 positive cell nucleus. (B) Quantification of proliferating cells at day 3 and 14. *$p < 0.05$. (C) HE staining displaying microvessels indicated by yellow arrows. (D) Quantification of microvessels at day 3, 14, and 28. *$p < 0.05$. (E) The total area of the microvessels in the grafts at day 3, 14, and 28. *$p < 0.05$. At early stages, the PHCS group showed less proliferating cells but higher microvessel number and area.

another side. At day 3, the total area of vessels in STSG grafts (2.68±0.49/HPF) was significantly lower than that in HCS (8.09±0.72/HPF) and PHCS grafts (13.75±0.20/HPF) ($p < 0.05$). While the vessel area increased in the STSG group overtime ($p < 0.05$), it decreased significantly in PHCS grafts at day 14 ($p < 0.05$) and reached a fairly stable status at day 28. Although the vessel area in HCS grafts was increased at day 14 (10.70±0.68/HPF) ($p < 0.05$), the growth trend was not pronounced at day 28 (12.97±0.97/HPF).

### Collagen deposition and maturation

Masson's trichrome staining and analysis was applied in order to depict collagen deposition and organization in the skin grafts (with the blue shaded area representing the collagen). As shown in Figure 7A, immature collagen (light blue, thin, and loosely packed) surrounded the fibroblasts in STSG grafts at day 28. While the collagen in HCS grafts was still in an admixed dysplastic state, mature collagen (bright blue, and densely packed) fibers were present in PHCS grafts at day 28. Quantitative image analysis (Figure 7B) demonstrated that the intensity of collagen deposition in STSG grafts (0.65 ± 0.01) was significantly lower than normal skin (0.71 ± 0.01) and HCS grafts (0.85 ± 0.02) ($p < 0.05$). Furthermore, the collagen level in PHCS grafts (0.70 ± 0.01) was closest to the normal skin collagen level.

## Discussion

In plastic and reconstructive surgery for treatment of deep burns, STSG transplantation is frequently chosen for a variety of situations when simple non-surgical wound care and skin flaps are inapplicable. However, partial or complete graft necrosis is a common problem of this surgical technique because it tends to induce severe contraction and fibrosis [46, 47]. Thus, the resulted scar tissue does not function like normal skin, as it does not contain the native skin structure such as hair follicles, sebaceous glands, and sensory nerve receptors [48]. Although various approaches for improving skin graft survival and decreasing contraction have been tried [49-54], problems still exist in promoting early vascularization of grafts and alleviating inflammation [55, 56] to regenerate durable and functional skin. hMSCs have been employed for treatment of full thickness wounds in different animal models. It was proposed that hMSCs participate in wound healing by functioning as: 1) trophic mediators to modulate T-cells, neutralize reactive oxygen species, and inhibit fibrosis; 2) progenitor cells transdifferentiating into multi-types of skin cells to promote tissue regeneration [7]. Many hMSC related studies have been conducted in immune compromised rodents [57-59], in which multiple skin transplantation models have been tried [60]. However, due to the importance of the immune system in wound healing [61, 62], an immune competent rat model was chosen in this study for the purpose of simulating healing processes in human wound repair [63]. Full-thickness excisional wounds with 20 mm diameter were created in the area between rats' scapular angles. Following full thickness skin excision, the HCS and PHCS samples were incorporated into the wound beneath the skin autograft. Skin graft contraction started around day 7 post surgery. Excess fibrosis, characterized by skin constriction and abnormal morphology, was found in the STSG group. The PHCS group had the lowest contraction ratio through 28 days, with morphology closest to the surrounding normal skin (Figure 3). This phenomenon is a reasonable result of a sequence of overlapping wound healing events including inflammatory response, neovascularization, proliferation, collagen deposition, and remodeling [64].

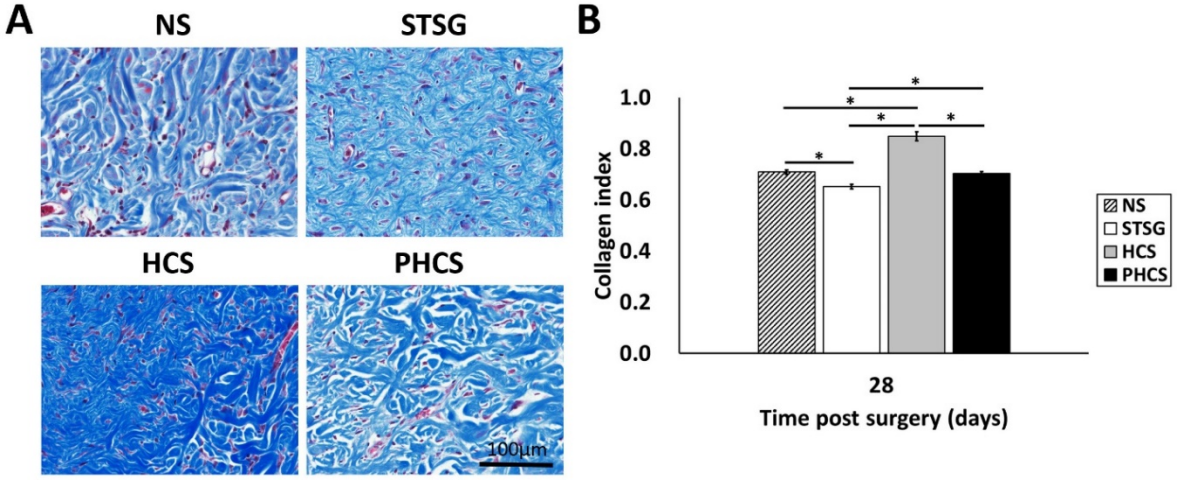

**Figure 7.** Collagen deposition in the skin graft and normal skin. (A) Masson's trichrome staining on post operational day 28. (B) Quantification of collagen intensity in the image. *$p < 0.05$. The morphology and intensity of collagen fibers in PHCS groups are closest to that of normal skin.

After implantation, the survival and status of grafts are critical to skin repair. The survival of skin grafts relies mainly on nutrient diffusion from the wound bed at the early stage of implantation [49, 65]. A large amount of various growth factors were preserved in the HCS grafts. Co-culture of ECs provided additional cytokines and growth factors that were also contained in the PHCS grafts (Figure 1). The presence of angiogenic factors in HCS and PHCS grafts can further stimulate the development of long-lasting functional neovasculature. The accumulation of red blood cells in the lumen of capillaries indicated the establishment of an efficacious blood circulation (Figure 6B), which supplies nutrients and removes waste from the grafts. The PHCS group had the highest vascularization level on day 3, which corresponded to the highest angiogenic factor levels. Significantly higher microvessel numbers and area in HCS and PHCS groups at this early stage was associated with an enhanced maintenance and viability of skin grafts. As opposed to its early stage, the high microvessel number and low microvessel area in the STSG group at a later stage implied that the vasculature was thin and immature. This phenomenon could be attributed to a persistent inflammation provoked by necrotic cells [66].

Inflammation is one of the critical wound healing phases. During this stage, inflammatory cells including neutrophils, macrophages, and mast cells arrive at the wound site to clear out dead cells, bacteria, and debris. However, the inflammation can lead to tissue damage if it lasts too long [67]. The acute inflammation stage usually lasts 72 hours. The disappearance of neutrophils in PHCS group at day 3 indicated limited tissue necrosis after implantation and on-going normal healing processes; whereas, the profuse presence of neutrophils in STSG and HCS groups suggested an excessively activated inflammatory response (Figure 4A and Figure S1), which may hinder the regeneration progress. Prior studies have shown that mast cells can release histamine, arachidonic acid metabolites, angiotensin II [68, 69], and cause hypertrophic scar contraction [70, 71]. At day 14 and 28 the mast cell number is significantly higher in the STSG group than in HCS and PHCS groups. Therefore, one of the reasons for significantly faster graft contraction rates of the STSG group was their much higher degree of mast cell infiltration compared to the other two groups (Figure S2).

Hair follicles, skin glands, and dermal collagen are important components for reconstitution of skin structure and function. Three days after implantation, the number of skin appendages, especially sebaceous glands, significantly decreased in STSG and HCS grafts. Simultaneously, collagen fibers were either degraded or went through necrosis, with slight hemorrhage. These phenomena were probably caused by surgical operation and insufficient blood supply [72]. The PHCS group had significantly improved performance compared to the other two groups. The graft structure and components (hair follicles and sebaceous glands) were better maintained from the beginning. At day 14, new skin appendages gradually appeared in STSG and HCS grafts but the recovery was much slower than in the PHCS group (Figure 4). These processes occurred along with the deposition and remodeling of collagen fibers.

At the end of our observation period (day 28), the histological appearance was significantly altered among the three groups. While the STSG group was the most fibrotic with thin, immature collagen deposition (Figure 7) and significant contraction, the HCS and PHCS groups showed much better recovery with the PHCS group returning to an approximately normal appearance. Dermis is mainly composed of collagen I, elastin, and fibrillin. The base membrane between dermis and epidermis is mainly composed of collagen IV, heparan sulfate proteoglycans, and fibronectin. It has been highlighted that the optimal composition of skin substitute scaffolds should mimic that of normal skin in order to enhance clinical effectiveness [73]. Both HCS and PHCS contain large amounts of ECM molecules including collagen I, collagen III, collagen IV, elastin, fibronectin, and laminin [26]. The pre-existing ECM components can accelerate the regeneration of dermal tissue. Our results suggest that imbedded cell sheets, especially PHCS, might have mitigated cellular processes associated with graft fibrosis and contraction.

Abnormal keratinocyte differentiation and their abnormal cytokine secretion are two factors demonstrated to contribute to tissue fibrosis and contraction by activating fibroblasts [74-76]. The epidermis maintained its original appearance in the PHCS group, and epidermal ulcers were soon covered with new, thin epidermis within 3 days in the HCS group; while the STSG group showed less recovery (Figure 5). The thickness of the neoepidermis in the STSG group increased significantly over time due to epidermal hyperplasia, a common response of dermal wounds characterized by overdevelopment of the epithelial cell layer. In contrast, HCS and PHCS epidermis maintained a below-trend change and quickly returned to their normal morphology. Since

the epidermis is the outmost layer of skin, a quick recovery of this layer can provide a barrier to infection from environmental pathogens and maintain water homeostasis inside the skin. However, excess epidermal hyperplasia results in dermal fibrosis and interferes with normal skin function [77]. The epidermis thickness was correspondent to the proliferating cells (Figure 6A) and neovasculature within dermal layer of the grafts. Proliferation and sufficient blood supply are necessary to rebuild new and healthy granulation tissue. However, in many cases the inflammatory stimulus tends to over-drive the proliferation leading to a pro-fibrotic response. The initial high cell proliferation and low vascularity in the STSG group were probably due to the fact that there was a greater need to replace necrotic cells in the tissue grafts that had less vascular support. The high cell proliferation in STSG persisted through the end of observation that corresponds to the high microvessel number in the tissue graft. The enhanced dermal cell proliferation level and hyperplastic STSG epidermis could play a role in grafts fibrosis and contraction [78]. Whereas, the presence of various cytokines and growth factors in the integrated cell sheet mediated the inflammation response in HCS and PHCS groups, which prevented the cell over-proliferation and microvessel over-growth.

Although we provided evidence to demonstrate the higher therapeutic efficiency of PHCS combined with autologous STSG implantation, some limitations still exist. Many studies support cell-replacement theory according to the observation that the transplanted hMSCs can respond to chemotactic signals *in vivo* [79] and transdifferentiate into correspondent cells such as endothelial cells, pericytes, and keratinocytes [80] to form new vessels or skin appendages through cellular reprogramming [32]. The hMSCs in cell sheets maintain a certain degree of progenicity and multi-lineage differentiation ability (Figure 2). It is possible that hMSCs responded to the *in vivo* environment and assumed a phenotype that resembles the resident skin cells including fibroblast, keratinocytes, and microvascular endothelial cells. Nonetheless, we only observed a small portion of surviving human cells (hMSCs/ECs) within HCS grafts at day 3 (Figure S3). Thus, the proliferating cells and microvessels we observed were mainly composed of rat cells. This finding is consistent with previous reports [81, 82] that the existence of hMSCs or ECs may not be necessary for the promotion of the healing process, but rather these cells appear to exert their therapeutic effects critically through the paracrine signaling molecules released by themselves [83-85]. In our study, the therapeutic result of different grafts was consistent with the growth factor levels in the cell sheets, suggesting that the paracrine activity may dominate the healing process in our full thickness wound model. Further studies are required to confirm this hypothesis and longer implantation time points are necessary to evaluate the complete remodeling process of the grafts.

## Conclusions

In conclusion, this study demonstrated that transplantation of autologous STSG along with HCS and PHCS significantly accelerated wound healing in a rat full thickness wound model. Both groups secreted angiogenic growth factors to regenerate the damaged tissue and support the construction of new blood vessels. Since ECs can secret more growth factors (ANG1 and ANG2), the PHCS group displayed the most effective paracrine activity. The PHCS group showed the smallest contraction, best preservation of skin appendages, highest number and area of microvessels, lowest inflammatory reactions, and a morphology that more closely resembles normal skin. The HCS and PHCS combined with STSG exhibited markedly enhanced therapeutic value in this rat model and may be useful for facilitating the healing of full thickness wound.

## Abbreviations

ANG1: angiopoietin 1
ANG2: angiopoietin 2
bFGF: basic fibroblast growth factor
CFU-F: colony-forming unit-fibroblast
DAPI: 4′, 6-diamidino-2-phenylindole
EC: endothelial cell
ECM: extracellular matrix
ELISA: enzyme-linked immunosorbent assay
FTG: full thickness graft
GM-CSF: granulocyte-macrophage colony-stimulating factor
HCS: human mesenchymal stem cell sheet
HE: hematoxylin and eosin
hMSC: human mesenchymal stem cell
HPF: high-power field
HUVECs: human umbilical vein endothelial cells
IHC: Immunohistochemistry
IL: interleukin
MSC: mesenchymal stem cell
NEM: n-ethylmaleimide
PDGF: platelet derived growth factor
PDGFR-α: platelet-derived growth factor receptor-α
PECAM-1: platelet/endothelial cell adhesion molecule-1
PFA: paraformaldehyde
PHCS: pre-vascularized hMSC sheet

PMSF: phenylmethylsulfonyl fluoride
SD: sprague dawley
STSG: split thickness skin grafting
TGF-$\beta$: transforming growth factor $\beta$
VEGF: vascular endothelial growth factor
vWf: von Willebrand factor

## Supplementary Material

Supplementary figures.
http://www.thno.org/v07p0117s1.pdf

## Acknowledgements

This study was supported by the National Institutes of Health (1R15CA202656 and 1R15HL115521-01A1) and the Portage Health Foundation Research Excellence Funds (PHF-REF) from Michigan Technological University to F.Z. It is also supported by the National Natural Science Foundation of China (NSFC: 81471883) to S.Q. and the Fundamental Research Funds for the Central Universities, Sun Yat-sen University (15ykjc10c) to L.C.

## Competing Interests

The authors have declared that no competing interest exists.

## References

1. Mendez-Eastman S. Burn injuries. Plast Surg Nurs. 2005; 25: 133-9.
2. Dreifke MB, Jayasuriya AA, Jayasuriya AC. Current wound healing procedures and potential care. Mater Sci Eng C Mater Biol Appl. 2015; 48: 651-62.
3. Shimizu R, Kishi K. Skin Graft. Plast Surg Int. 2012; 2012: 563493.
4. Wood FM. Skin regeneration: The complexities of translation into clinical practise. Int J Biochem Cell Biol. 2014; 56: 133-40.
5. Zografou A, Papadopoulos O, Tsigris C, Kavantzas N, Michalopoulos E, Chatzistamatiou T, et al. Autologous transplantation of adipose-derived stem cells enhances skin graft survival and wound healing in diabetic rats. Ann Plast Surg. 2013; 71: 225-32.
6. Halim AS, Khoo TL, Yussof SJ. Biologic and synthetic skin substitutes: An overview. Indian J Plast Surg. 2010; 43: S23-S8.
7. Jackson WM, Nesti LJ, Tuan RS. Mesenchymal stem cell therapy for attenuation of scar formation during wound healing. Stem Cell Res Ther. 2012; 3: 20.
8. Caplan AI. Adult mesenchymal stem cells for tissue engineering versus regenerative medicine. J Cell Physiol. 2007; 213: 341-7.
9. Fu X, Fang L, Li X, Cheng B, Sheng Z. Enhanced wound-healing quality with bone marrow mesenchymal stem cells autografting after skin injury. Wound Repair Regen. 2006; 14: 325-35.
10. Balaji S, Keswani SG, Crombleholme TM. The role of mesenchymal stem cells in the regenerative wound healing phenotype. Adv Wound Care. 2012; 1: 159-65.
11. Nemos C, Basciano L, Dalloul A. Biological effects and potential applications of mesenchymal stem cell culture under low oxygen pressure. Pathol Biol (Paris). 2012; 60: 193-8.
12. Deng W, Han Q, Liao L, Li C, Ge W, Zhao Z, et al. Engrafted bone marrow-derived flk-(1+) mesenchymal stem cells regenerate skin tissue. Tissue Eng. 2005; 11: 110-9.
13. Nie C, Yang D, Xu J, Si Z, Jin X, Zhang J. Locally administered adipose-derived stem cells accelerate wound healing through differentiation and vasculogenesis. Cell Transplant. 2011; 20: 205-16.
14. Shin L, Peterson DA. Human mesenchymal stem cell grafts enhance normal and impaired wound healing by recruiting existing endogenous tissue stem/progenitor cells. Stem Cells Transl Med. 2013; 2: 33-42.
15. Yang J, Yamato M, Nishida K, Ohki T, Kanzaki M, Sekine H, et al. Cell delivery in regenerative medicine: The cell sheet engineering approach. J Control Release. 2006; 116: 193-203.
16. Yamato M, Utsumi M, Kushida A, Konno C, Kikuchi A, Okano T. Thermo-responsive culture dishes allow the intact harvest of multilayered keratinocyte sheets without dispase by reducing temperature. Tissue Eng. 2001; 7: 473-80.
17. Kato Y, Iwata T, Morikawa S, Yamato M, Okano T, Uchigata Y. Allogeneic transplantation of an adipose-derived stem cell sheet combined with artificial skin accelerates wound healing in a rat wound model of type 2 diabetes and obesity. Diabetes. 2015; 64: 2723-34.
18. Seyhan T. Split-thickness skin grafts. In: Spear M, editor. Skin Grafts - Indications, Applications and Current Research: InTech; 2011.
19. Chua AWC, Khoo YC, Tan BK, Tan KC, Foo CL, Chong SJ. Skin tissue engineering advances in severe burns: review and therapeutic applications. Burns & Trauma. 2016; 4.
20. Kang Y, Ren L, Yang Y. Engineering vascularized bone grafts by integrating a biomimetic periosteum and beta-TCP scaffold. ACS Appl Mater Interfaces. 2014; 6: 9622-33.
21. Lesman A, Habib M, Caspi O, Gepstein A, Arbel G, Levenberg S, et al. Transplantation of a tissue-engineered human vascularized cardiac muscle. Tissue Eng Part A. 2010; 16: 115-25.
22. Mantovani A, Bussolino F, Dejana E. Cytokine regulation of endothelial-cell function. FASEB J. 1992; 6: 2591-9.
23. Mendes LF, Pirraco RP, Szymczyk W, Frias AM, Santos TC, Reis RL, et al. Perivascular-like cells contribute to the stability of the vascular network of osteogenic tissue formed from cell sheet-based constructs. PLoS One. 2012; 7.
24. Xue Y, Xing Z, Bolstad AI, Van Dyke TE, Mustafa K. Co-culture of human bone marrow stromal cells with endothelial cells alters gene expression profiles. Int J Artif Organs. 2013; 36: 650-62.
25. Li Q, Wang Z. Influence of mesenchymal stem cells with endothelial progenitor cells in co-culture on osteogenesis and angiogenesis: an in vitro study. Arch Med Res. 2013; 44: 504-13.
26. Zhang L, Xing Q, Qian Z, Tahtinen M, Zhang Z, Shearier E, et al. Hypoxia created human mesenchymal stem cell sheet for prevascularized 3D tissue construction. Adv Healthc Mater. 2016; 5: 342-52.
27. Reing J, Brown B, Daly K, Freund J, Gilbert T, Hsiong S, et al. The effects of processing methods upon mechanical and biologic properties of porcine dermal extracellular matrix scaffolds. Biomaterials. 2010; 31: 8626-33.
28. Zhao F, Grayson WL, Ma T, Bunnell B, Lu WW. Effects of hydroxyapatite in 3-D chitosan-gelatin polymer network on human mesenchymal stem cell construct development. Biomaterials. 2006; 27: 1859-67.
29. Xing Q, Qian Z, Kannan B, Tahtinen M, Zhao F. Osteogenic differentiation evaluation of an engineered extracellular matrix based tissue sheet for potential periosteum replacement. ACS Appl Mater Interfaces. 2015; 7: 23239-47.
30. Kim J, Ma T. Autocrine fibroblast growth factor 2-mediated interactions between human mesenchymal stem cells and the extracellular matrix under varying oxygen tension. J Cell Biochem. 2013; 114: 716-27.
31. Liu Y, Huang XY, Yang XH. Experimental study of autologous skin grafting on retained denatured dermis for the treatment of partial thickness burn wound. Zhonghua Shao Shang Za Zhi. 2005; 21: 14-6.
32. Ibrahim MM, Bond J, Bergeron A, Miller KJ, Ehanire T, Quiles C, et al. A novel immune competent murine hypertrophic scar contracture model: a tool to elucidate disease mechanism and develop new therapies. Wound Repair Regen. 2014; 22: 755-64.
33. Ibrahim MM, Chen L, Bond JE, Medina MA, Ren L, Kokosis G, et al. Myofibroblasts contribute to but are not necessary for wound contraction. Lab Invest. 2015; 95: 1429-38.
34. Svensjo T, Pomahac B, Yao F, Slama J, Eriksson E. Accelerated healing of full-thickness skin wounds in a wet environment. Plast Reconstr Surg. 2000; 106: 602-12; discussion 13-4.
35. Olbrich KC, Meade R, Bruno W, Heller L, Klitzman B, Levin LS. Halofuginone inhibits collagen deposition in fibrous capsules around implants. Annals of plastic surgery. 2005; 54: 293-6;discussion 6.
36. Kyriakides TR, Wulsin D, Skokos EA, Fleckman P, Pirrone A, Shipley JM, et al. Mice that lack matrix metalloproteinase-9 display delayed wound healing associated with delayed reepithelization and disordered collagen fibrillogenesis. Matrix Biol. 2009; 28: 65-73.
37. Javazon EH, Keswani SG, Badillo AT, Crombleholme TM, Zoltick PW, Radu AP, et al. Enhanced epithelial gap closure and increased angiogenesis in wounds of diabetic mice treated with adult murine bone marrow stromal progenitor cells. Wound Repair Regen. 2007; 15: 350-9.
38. Di-Poi N, Ng CY, Tan NS, Yang Z, Hemmings BA, Desvergne B, et al. Epithelium-mesenchyme interactions control the activity of peroxisome proliferator-activated receptor beta/delta during hair follicle development. Mol Cell Biol. 2005; 25: 1696-712.
39. Donoghue JF, McGavigan CJ, Lederman FL, Cann LM, Fu L, Dimitriadis E, et al. Dilated thin-walled blood and lymphatic vessels in human endometrium: a potential role for VEGF-D in progestin-induced break-through bleeding. PLoS One. 2012; 7: e30916.
40. Zisch A, Lutolf M, Hubbell J. Biopolymeric delivery matrices for angiogenic growth factors. Cardiovascular pathology. 2003; 12: 295-310.
41. Goumans MJ, Valdimarsdottir G, Itoh S, Rosendahl A, Sideras P, ten Dijke P. Balancing the activation state of the endothelium via two distinct TGF-beta type I receptors. EMBO J. 2002; 21: 1743-53.
42. Yancopoulos GD, Davis S, Gale NW, Rudge JS, Wiegand SJ, Holash J. Vascular-specific growth factors and blood vessel formation. Nature. 2000; 407: 242-8.

43. Augustin HG, Koh GY, Thurston G, Alitalo K. Control of vascular morphogenesis and homeostasis through the angiopoietin-Tie system. Nat Rev Mol Cell Biol. 2009; 10: 165-77.
44. Garbuzenko E, Nagler A, Pickholtz D, Gillery P, Reich R, Maquart FX, et al. Human mast cells stimulate fibroblast proliferation, collagen synthesis and lattice contraction: a direct role for mast cells in skin fibrosis. Clin Exp Allergy. 2002; 32: 237-46.
45. Broughton G, Janis JE, Attinger CE. The basic science of wound healing. Plast Reconstr Surg. 2006; 117: 12S-34S.
46. Ratner D. Skin grafting. Seminars in cutaneous medicine and surgery. 2003; 22: 295-305.
47. MacFarlane DF. Current techniques in skin grafting. Adv Dermatol. 2006; 22: 125-38.
48. Martin P. Wound healing - Aiming for perfect skin regeneration. Science. 1997; 276: 75-81.
49. Azzopardi EA, Boyce DE, Dickson WA, Azzopardi E, Laing JH, Whitaker IS, et al. Application of topical negative pressure (vacuum-assisted closure) to split-thickness skin grafts: a structured evidence-based review. Ann Plast Surg. 2013; 70: 23-9.
50. Eckhaus AA, Fish JS, Skarja G, Semple JL, Sefton MV. A preliminary study of the effect of poly(methacrylic acid-co-methyl methacrylate) beads on angiogenesis in rodent skin grafts and the quality of the panniculus carnosus. Plast Reconstr Surg. 2008; 122: 1361-70.
51. Zarifkar A, Habibi H, Namazi MR, Hosseininasab SJ, Mosavat SH, Khatibi A, et al. Administration of heparanase-III improves the survival and angiogenesis of rat skin autografts. G Ital Dermatol Venereol. 2009; 144: 195-8.
52. Isenberg JS, Pappan LK, Romeo MJ, Abu-Asab M, Tsokos M, Wink DA, et al. Blockade of thrombospondin-1-CD47 interactions prevents necrosis of full thickness skin grafts. Ann Surg. 2008; 247: 180-90.
53. Currie LJ, Sharpe JR, Martin R. The use of fibrin glue in skin grafts and tissue-engineered skin replacements: a review. Plast Reconstr Surg. 2001; 108: 1713-26.
54. Zhang F, Oswald TM, Lin L, Wang S, Lin S, Lineaweaver WC. Improvement of full-thickness skin graft survival by application of vascular endothelial growth factor in rats. Ann Plast Surg. 2008; 60: 589-93.
55. Motsch B, Heim C, Koch N, Ramsperger-Gleixner M, Weyand M, Ensminger SM. Microvascular integrity plays an important role for graft survival after experimental skin transplantation. Transpl Immunol. 2015; 33: 204-9.
56. Delaney TA, Morehouse C, Brohawn PZ, Groves C, Colonna M, Yao Y, et al. Type I IFNs regulate inflammation, vasculopathy, and fibrosis in chronic cutaneous graft-versus-host disease. J Immunol. 2016; 197: 42-50.
57. Gamblin AL, Brennan MA, Renaud A, Yagita H, Lezot F, Heymann D, et al. Bone tissue formation with human mesenchymal stem cells and biphasic calcium phosphate ceramics: the local implication of osteoclasts and macrophages. Biomaterials. 2014; 35: 9660-7.
58. Re'em T, Kaminer-Israeli Y, Ruvinov E, Cohen S. Chondrogenesis of hMSC in affinity-bound TGF-beta scaffolds. Biomaterials. 2012; 33: 751-61.
59. Frescaline G, Bouderlique T, Mansoor L, Carpentier G, Baroukh B, Sineriz F, et al. Glycosaminoglycan mimetic associated to human mesenchymal stem cell-based scaffolds inhibit ectopic bone formation, but induce angiogenesis in vivo. Tissue Eng Part A. 2013; 19: 1641-53.
60. Hamuy R, Kinoshita N, Yoshimoto H, Hayashida K, Houbara S, Nakashima M, et al. One-stage, simultaneous skin grafting with artificial dermis and basic fibroblast growth factor successfully improves elasticity with maturation of scar formation. Wound Repair Regen. 2013; 21: 141-54.
61. Portou MJ, Baker D, Abraham D, Tsui J. The innate immune system, toll-like receptors and dermal wound healing: A review. Vascul Pharmacol. 2015; 71: 31-6.
62. Sun BK, Siprashvili Z, Khavari PA. Advances in skin grafting and treatment of cutaneous wounds. Science. 2014; 346: 941-5.
63. Rose LF, Wu JC, Carlsson AH, Tucker DI, Leung KP, Chan RK. Recipient wound bed characteristics affect scarring and skin graft contraction. Wound Repair Regen. 2015; 23: 287-96.
64. Martin P. Wound healing--aiming for perfect skin regeneration. Science. 1997; 276: 75-81.
65. Horch RE, Bannasch H, Stark GB. Transplantation of cultured autologous keratinocytes in fibrin sealant biomatrix to resurface chronic wounds. Transplant Proc. 2001; 33: 642-4.
66. Aarabi S, Longaker MT, Gurtner GC. Hypertrophic Scar Formation Following Burns and Trauma: New Approaches to Treatment. PLoS Med. 2007; 4: e234.
67. Midwood KS, Williams LV, Schwarzbauer JE. Tissue repair and the dynamics of the extracellular matrix. Int J Biochem Cell Biol. 2004; 36: 1031-7.
68. Hara M, Ono K, Wada H, Sasayama S, Matsumori A. Preformed angiotensin II is present in human mast cells. Cardiovasc Drugs Ther. 2004; 18: 415-20.
69. Bond JE, Bergeron A, Thurlow P, Selim MA, Bowers EV, Kuang A, et al. Angiotensin-II mediates nonmuscle myosin II activation and expression and contributes to human keloid disease progression. Mol Med. 2011; 17: 1196-203.
70. Kischer CW, Bunce H, 3rd, Shetlah MR. Mast cell analyses in hypertrophic scars, hypertrophic scars treated with pressure and mature scars. J Invest Dermatol. 1978; 70: 355-7.
71. Foley TT, Saggers GC, Moyer KE, Ehrlich HP. Rat mast cells enhance fibroblast proliferation and fibroblast-populated collagen lattice contraction through gap junctional intercellular communications. Plast Reconstr Surg. 2011; 127: 1478-86.
72. Manske RC. Postsurgical orthopedic sports rehabilitation- knee & shoulder. MOSBY ELSEVIER; 2006.
73. Markeson D, Pleat JM, Sharpe JR, Harris AL, Seifalian AM, Watt SM. Scarring, stem cells, scaffolds and skin repair. J Tissue Eng Regen Med. 2015; 9: 649-68.
74. Peura M, Siltanen A, Saarinen I, Soots A, Bizik J, Vuola J, et al. Paracrine factors from fibroblast aggregates in a fibrin-matrix carrier enhance keratinocyte viability and migration. J Biomed Mater Res A. 2010; 95: 658-64.
75. Amjad SB, Carachi R, Edward M. Keratinocyte regulation of TGF-beta and connective tissue growth factor expression: a role in suppression of scar tissue formation. Wound Repair Regen. 2007; 15: 748-55.
76. Li B, Gao C, Diao JS, Wang DL, Chu FF, Li Y, et al. Aberrant Notch signalling contributes to hypertrophic scar formation by modulating the phenotype of keratinocytes. Exp Dermatol. 2016; 25: 137-42.
77. Neary R, Watson CJ, Baugh JA. Epigenetics and the overhealing wound: the role of DNA methylation in fibrosis. Fibrogenesis Tissue Repair. 2015; 8: 18.
78. Lupher ML, Jr., Gallatin WM. Regulation of fibrosis by the immune system. Adv Immunol. 2006; 89: 245-88.
79. Newman RE, Yoo D, LeRoux MA, Danilkovitch-Miagkova A. Treatment of inflammatory diseases with mesenchymal stem cells. Inflamm Allergy Drug Targets. 2009; 8: 110-23.
80. Sasaki M, Abe R, Fujita Y, Ando S, Inokuma D, Shimizu H. Mesenchymal stem cells are recruited into wounded skin and contribute to wound repair by transdifferentiation into multiple skin cell type. J Immunol. 2008; 180: 2581-7.
81. Rosario CM, Yandava BD, Kosaras B, Zurakowski D, Sidman RL, Snyder EY. Differentiation of engrafted multipotent neural progenitors towards replacement of missing granule neurons in meander tail cerebellum may help determine the locus of mutant gene action. Development. 1997; 124: 4213-24.
82. Li TS, Takahashi M, Ohshima M, Qin SL, Kubo M, Muramatsu K, et al. Myocardial repair achieved by the intramyocardial implantation of adult cardiomyocytes in combination with bone marrow cells. Cell Transplant. 2008; 17: 695-703.
83. Hocking AM, Gibran NS. Mesenchymal stem cells: paracrine signaling and differentiation during cutaneous wound repair. Exp Cell Res. 2010; 316: 2213-9.
84. Lee EY, Xia Y, Kim WS, Kim MH, Kim TH, Kim KJ, et al. Hypoxia-enhanced wound-healing function of adipose-derived stem cells: increase in stem cell proliferation and up-regulation of VEGF and bFGF. Wound Repair Regen. 2009; 17: 540-7.
85. Chen L, Xu Y, Zhao J, Zhang Z, Yang R, Xie J, et al. Conditioned medium from hypoxic bone marrow-derived mesenchymal stem cells enhances wound healing in mice. PloS one. 2014; 9: e96161.